Analysis of Spatially Modelled High Temperature Polymer Electrolyte Membrane Fuel Cell under Dynamic Load Conditions

Jagdesh Kumar[1]
School of Technology and Innovations
University of Vaasa, Finland, Department of Electrical
Engineering, Quaid-e-Awam
University of Engineering Science & Technology, (QUEST)
Nawabshah, 67480, Sindh, Pakistan

Jherna Devi[2]
Institute of Technology for Nanostructures (NST) and
Center for Nano Integration Duisburg-Essen (CENIDE),
University Duisburg-Essen, Duisburg D-47057, Germany,
Department of Information Technology, Quaid-e-Awam
University of Engineering Science & Technology, (QUEST)
Nawabshah, 67480, Sindh, Pakistan

Ghulam Mustafa Bhutto[3]
Department of Electrical Engineering, Quaid-e-Awam
University of Engineering Science & Technology, (QUEST)
Nawabshah, 67480, Sindh, Pakistan

Sajida Parveen[4]
Department of Computer Systems Engineering, Quaid-e-
Awam University of Engineering Science & Technology,
(QUEST) Nawabshah, 67480, Sindh, Pakistan

Muhammad Shafiq[5]
School of Technology and Innovations
University of Vaasa, Finland

Abstract—**This paper presents an interesting approach to observe the effects of the load variations on the performance of high temperature polymer electrolyte membrane fuel cell system, such as: hydrogen and air flow rate, output voltage, power and efficiency. The main advantage of this approach is to analyse the internal behaviour of the fuel cell like current-voltage characteristics during energy conversion, when the load is varying dynamically. This approach of power system simulation models fuel cell system by integrating 3D-COMSOL model of high temperature polymer electrolyte membrane fuel cell with MATLAB/Simulink model of the fuel cell system. The MATLAB/Simulink model for the fuel cell system includes the fuel cell stack (single cell), load (sequence of currents), air supply system (air compressor), fuel supply system (hydrogen tank), and power-efficiency block. The MATLAB/Simulink model is developed in such a way that one part behaves as an input model to the 3D-COMSOL model of the fuel cell system, whereas second part behaves as an output model that recovers the results obtained from the 3D-COMSOL of the fuel cell. This approach of power system modelling is useful to show the performance of high temperature polymer electrolyte membrane fuel cell in much better and accurate way.**

Keywords—Current-voltage characteristics; energy conversion; fuel cells; power system modeling; power system simulation

I. INTRODUCTION

The exponential growth in electricity demand, depletion in fossil fuel and production of environmental pollutions, global concerns regarding environmental pollution, and deregulation in the electrical power market have driven the application of distributed energy resources to experience a boost in the power systems as a mean of producing electrical energy [1]–[6]. A Distributed generation (DG) is available in different forms, which provide the customers a wide range of costs and reliability. A DG technology commonly consists of micro-scale to large-scale power generating resources [7] [8], like small gas turbines, micro turbines, mini hydro, bio-mass, wind, photovoltaic, and fuel cells. Among the distributed energy sources, fuel cells having high power density have gained a great attraction due to its environment friendly operation and can be promising alternative for internal combustion engines [9]. It can be a suitable and an economical option for rural electrification in developing countries.

A fuel cell energy is the results of an electrochemical process in which chemical energy of reaction is directly converted into electrical energy. The popularity of fuel cells as a mean for producing electrical energy increased from last two decade due to many advantages possessed by them. Fuel cells developed today are frequently used in zero-emission electric transportation of vehicles and vessels, off-grid and distributed power generation and in portable consumer electronics [2] [5] [9]-[13]. The wide range applications of fuel cell power system varies from few watts to megawatts make them unique energy converters as compared to any other energy conversion technology. Fuel cells have many characteristics such as they are environmental friendly because they do not use fossil fuels and hence do not produce emissions. They have higher efficiency in the range of 60-80%, they require low maintenance because they are static source of electric power [14] [15] they have comparatively higher efficiency than diesel or gas engines and operate noiselessly. They are sometimes more suitable than batteries because they provide continuous supply of electric power whereas the batteries face the charging and discharging processes. Fuel cells are categorised into different types based on electrolytes, cell material, operating

temperature, and fuel diversity. High Temperature Polymer Electrolyte Membrane Fuel Cell (HT-PEMFC) is considered to be the next generation fuel cell [16], because the electrochemical kinetics for electrode reactions is enhanced as compared to Low Temperature Polymer Electrolyte Membrane Fuel Cell (LT-PEMFC). The HT-PEMFC uses phosphoric acid doped polymer membranes and typically operates above 120°C up to 200°C [5].

LT-PEMFC is already a well-established technology whereas a little research work has been done so far on the development of HTPEMFC system. Despite many advantages, the main problem lies in the modelling of fuel cell to analyse their behaviour. Mathematical models for the fuel cells have attained a great attention in recent years. In [17], PEMFC mathematical model is developed with MATLAB/Simulink and the results are compared with the real test system. It has been found that the developed model is suitable to predict characteristics of the fuel cell as well as analyse, design optimization and real-time control of the PEMFCs. The performance of PEMFC under a constant current and constant power mode has also been analysed and different characteristics have been experimentally found and compared with theoretical calculation in [18]. The semi-empirical model of HT-PEMFC is developed in [19], which can predict the dynamic response at various random loads and fuzzy controller is designed or scheduling the purging process. The performance of 3D-COMSOL model of HT-PEMFC, based on three parameters: operating temperature, catalyst layer thickness, and proton exchange membrane thickness, has been investigated in [20]. The PEMFC having high energy density has been used in different hybrid energy systems and different control algorithms have been applied for optimal and efficient use of energy storage systems [14] [21] [22]. The several methods of starting up of HT-PEMFC from room temperature to the operating temperature are investigated in [23].

The most of the modelling of fuel cell are used in MATLAB/Simulink or COMSOL environment separately. These separate modelling in separate simulation tools has their own relative merits and demerits. COMSOL has the advantage that it can show the internal behaviours of the fuel cell. However, it has limitation that it cannot provide a facility to test fuel cell for dynamic load variations. On the other hand, MATLAB/Simulink has the ability to change the various parameters of the fuel cell but internal behaviours cannot be observed. To address this issue, this paper propose a new method which aims to identify the effect of load variation on performance of the HT-PEMFC by integrating HT-PEMFC model of COMSOL with the fuel cell system model of the MATLAB/Simulink by using MATLAB programming. This approach is suitable to find the internal behaviour of the HT-PEMFC while analysing the variation in load. The rest of the paper is organised as follows: Section II explains methodology of modelling the HT-PEMFC system, Section III presents the results obtained by the MATLAB/Simulink as well as COMSOL, and Section IV presents conclusion and future work follow.

II. MODELLING OF HT-PEMFC SYSTEM

This section describes the modelling of HT-PEMFC system that consists of HT-PEM fuel cell (fuel cell stack), load profile (sequence of currents), air supply system (air compressor), H2 supply (hydrogen tank), and power block for measuring total power, net power and hence the efficiency. All the subsystems of HT-PEMFC system are modelled in MATLAB/Simulink, except HT-PEM fuel cell for which 3D-COMSOL model is used. Subsections A, B, and C explain in detail the MATLAB/Simulink modelling, 3D-COMSOL modelling and integration of MATLAB/Simulink model with 3D-COMSOL model respectively.

A. HT-PEMFC System Model in MATLAB/Simulink

The objective of the MATLAB Simulink model is to observe the effects of the load variation on HT-PEMFC performance, output power and efficiency as well as to regulate HT-PEMFC system dynamically to meet the desired load variations. The following are the subsystems are used to model the fuel cell system model.

1) Air supply system: A good performance of a fuel cell stack is based on the required air mass flow rate and air pressure. The mass flow rate and the pressure of the air in many fuel cell system designs are varied to control the oxygen partial pressure, depending on the electrical power output required from the fuel cell stack. The energy requirement of compression process is the main part of the energy consumption of the auxiliary systems in fuel cell system. A realistic air supply model is necessary for use in fuel cell system development particularly for two reasons. First for accurately analysing the fuel cell system performance. Secondly, it is important for maximizing the performance of a particular fuel cell system configuration. The Mass flow rate (kg/sec) of air is changed in this model in accordance with the dynamic variation in load current. The air flow rate in litter per minute is calculated by the equation (1).

$$V_{lpm(air)} = \frac{60000RT \, i_{fc}}{U_{f(O2)}zFP_{(air)}y\%} \tag{1}$$

Where,

R: Universal gas constant, 8.3145 [J·mol^{-1}·K^{-1}],

T: Operating temperature, 453.13 [K],

i_{fc}: fuel cell operating current, [A]

$U_{f(O2)}$: Oxygen utilization [set to be 0.593],

z: Number of moving electrons 2 for hydrogen,

F: Faraday's constant, 96485 [A·s·mol^{-1}],

$P_{(air)}$: Air Pressure 1.1 [bar]

$y\%$: Air composition [set to be 0.21]

As in this model, the air pressure is varied with respect to the mass flow rate in kg/sec, so we have to convert this expression considering the air density of air as 1.225 kg/m³ (sea level, 15°C).

The pressure ratio of an air varies in accordance with the mass flow rate and in this model; a look up table is used to evaluate the pressure ratio by considering the values of mass flow rate and pressure ratio from the compressor performance map. The minimum and maximum set points for mass flow rate are used as 1e-7 and 0.09 kg/sec respectively by considering the values used in look up table. In the same way, the minimum and maximum values for pressure ratio used are 1.1 and 4. Here one thing is very important to notice that minimum set point value of pressure ratio should be greater than 1. Otherwise, power consumption by the air compressor will be zero at pressure ratio equal to one.

In an adiabatic (no heat loss), the pressure changes from P2 to P1, then the temperature will change from T1 to T2' as shown in equation (2).

$$T_2{}' = T_1 \left(\frac{P_2}{P_1}\right)^{(\gamma-1)/\gamma} \tag{2}$$

Where, Υ is the ratio of the specific heat capacities of the gas that is Cp/Cv and its value is 1.4 at 20°C. Where P1 and T1 are the applied pressure and temperature of the incoming air that are 1.1 bar and 298 K and P2 is the output pressure of the air compressor.

The actual temperature change will be higher than the isentropic temperature change because some of the motion of the moving blades and vanes in compressor can raise the temperature of the gas. It can be obtained by using the following equation (3).

$$\Delta T = T_2 - T_1 = \frac{T_1}{\eta_c} \left(\left(\frac{P_2}{P_1}\right)^{\frac{\gamma-1}{\gamma}} - 1\right) \tag{3}$$

Where η_c: Compressor efficiency [%]

Keeping in view, the safe operation and optimum efficiency, a look up table is used to obtain the compressor efficiency in correspondence with the pressure ratio.

The power consumed to drive a compressor can be easily calculated from the change in temperature by using the equation (4).

$$Power = W' = Cp\Delta T m' \tag{4}$$

Where m' is the mass flow rate in kg/sec, and change in temperature ΔT can be obtained by using equation (3) , so we have another equation in terms of pressure ratio as shown in equation (5).

$$Power = Cp \frac{T1}{\eta_c} \left(\left(\frac{P2}{P1}\right)^{(\gamma-1)/\gamma} - 1\right) m' \tag{5}$$

Where,

Cp: 1004 [J·Kg^{-1}·K^{-1}]

Υ: 1.4

η_c: Isentropic efficiency

To find the power needed from the motor or turbine driving the compressor, the equation 5 is divided by the mechanical efficiency η_m, which is taken 0.98 in this model.

2) Fuel supply system (Hydrogen Tank): The hydrogen is fed to the anode in dead ended mode, so that there is no venting or circulation of the gas, but it is consumed by the fuel cell. The hydrogen is supposed to be stored in a tank at a pressure of 300 bars. It can be further reduced through the pressure reduction valves to a value comparable to the compressed air pressure that is approximately in the range of 1.1 to 4 bars as mentioned in the earlier section.

The anode inlet flow rate can be adjusted instantaneously by a valve to keep the pressure difference between the cathode and anode as minimum as possible. Here it is supposed that the anode flow resistance is negligible as compared to the cathode flow so that pressure difference can be maintained for the sufficient amount of flow of hydrogen for fuel cell reaction. The temperature of flow is supposed to be equal to the fuel cell temperature and the condition of the gas namely pressure, temperature of anode outlet flow is the same as the condition of the gas in the anode flow channel. The partial pressure of hydrogen can be determined by balancing the mass flow of hydrogen in anode. The model contains anode inlet total mass m_{H2_in}, inlet flow pressure $p_{H2,in}$, inlet flow temperature $T_{an,in}$, fuel cell current I_{st} ,fuel cell temperature T_{st} . The state of hydrogen mass m_{H2_an} inside the anode volume can be obtained by equation 6.

$$\frac{dm_{H_2\_an}}{dt} = \dot{m}_{H_2\_an\_in} - \dot{m}_{H_2 reacted} \tag{6}$$

The other parameter of mass balance equation is to calculate the consumed hydrogen reaction rate is function of stack current given by equation 7.

$$\dot{m}_{H_2\_react} = M_{H_2} \cdot \frac{N_{cell} \cdot I_{st}}{2F} \tag{7}$$

The mass of hydrogen calculated is used to determine hydrogen partial pressure $p_{H2,an}$ given by equation 8.

$$p_{H_2,an} = \frac{m_{H_2\_an} \cdot R_{H_2} \cdot T_{opr}}{V_{an}} \tag{8}$$

Whereas, the anode pressure is given by equation 9.

$$p_{an} = p_{H_2,an} \tag{9}$$

The mass flow rate of hydrogen is controlled by at anode inlet by proportional control, which follows the changes in cathode pressure (p_{ca}) and given by equation 10.

$$\dot{m}_{an\_in} = k_1 \cdot (p_{ca} - p_{an}) \tag{10}$$

Table I represents the physical parameters, which are used in the equations of hydrogen fuel supply.

TABLE I. PHYSICAL PARAMETERS OF HYDROGEN GAS

Symbol	Definition	Value
R_{H_2}	Hydrogen gas constant	8.3145 J·mol^{-1}·K^{-1}
T_{opr}	Operating temperature	453.13 K
V_{an}	Anode volume	0.005 m³
M_{H_2}	Hydrogen molar mass	2.016e-3 Kg/mole
N_{cell}	Number of cell in fuel cell stack	1
F	Faraday constant	96485 C/mole
k_1	Proportional gain for the supply valve	2.1 Kg/(s·kPa)

The fuel flow rate of hydrogen is changed in accordance with the dynamic variation in load current. The fuel flow rate is in litre per minute and calculated by the equation 11.

$$V_{lpm(fuel)} = \frac{60000RTifc}{U_{f(H2)}zFP_{(fuel)}x\%} \tag{11}$$

Where:

R: Universal gas constant, 8.3145 [J·mol^{-1}·K^{-1}],

T: Operating temperature, 453.13 [K],

i_{fc}: fuel cell operating current, [A]

$U_{f(H2)}$: Hydrogen utilization [set to be 0.99556],

z: Number of moving electrons 2 for hydrogen,

F: Faraday's constant, 96485 [A.s.mol^{-1}],

$P_{(fuel)}$: Fuel pressure , calculated from equation 8,

$X\%$: Hydrogen composition [set to be 0.9995]

In this model, hydrogen stored in a tank is considered at a pressure of 300 bar and at ambient room temperature of 298 K. Now adiabatic changes in output temperature T2' can be found by using equation 12.

$$T_2{}' = T_1 \left(\frac{P_2}{P_1}\right)^{(\gamma-1)/\gamma} \tag{12}$$

Where:

T_1: 298 K for hydrogen to be at room temperature

γ: Cp/Cv= 1.405 for hydrogen

P_1: 300 bar

P_2: Partial pressure of hydrogen (P_f)

3) Dynamic load profile: The load in the model is considered as sequence of currents applied at different time steps. The total time of simulation is 4 seconds with the 400 time steps, means each time step is of 0.01 second and the value of the load current is assigned to each time step. The sequence of current is applied in such a way that for each 80-time steps the load current is changed. For the first 80 time steps, the load current 0.06 A is considered, and for the remaining each 80 steps 0.04 A, 0.05 A, 0.07 A, and 0.03 A of the load current is considered.

4) Power block: The power block is used to measure fuel cell input and output power, net power, and the overall system efficiency. The Stack power is also known as output power obtained from the fuel cell. It is defined as the product of fuel cell voltage and the current drawn by the load from the fuel cell. It is given by equation 13.

$$P_{out} = V_{cell}I_{load} \tag{13}$$

The input power of the fuel cell is obtained by dividing fuel cell output power divided by the fuel cell stack efficiency, given by the equation 14.

$$P_{in} = \frac{P_{out}}{\eta_{stack}} \tag{14}$$

Where η_{stack} is fuel cell stack efficiency and given by the equation 15.

$$\eta_{stack=} \left(\frac{N_c \cdot I_{fc}}{ZFU_{fH2}}\right) \cdot \Delta_{Ho} \tag{15}$$

Where

N_c: Number of cells=1;

I_{fc}: Fuel cell current;

z: Number of moving electrons=2;

U_{fH2}: Utilization of hydrogen,

Δ_{HO}: Reaction Enthalpy, [241830 J·mol^{-1}]

The net power obtained from the fuel cell stack is equal to the total stack power generated minus the power consumed by auxiliary equipment. In this model, the air compressor is used as auxiliary equipment that consumes the power, so the net power here will be the total power minus the compressor power given by equation 16.

$$P_{net} = P_{out} - P_{comp} \tag{16}$$

Thus, the overall fuel cell system efficiency is in this model is obtained by simply dividing the net power Pnet by the total power input Pin to the fuel cell stack.

B. Spatial modelling of HT-PEMFC in COMSOL

COMSOL is a flexible platform that allows users to model all relevant physical aspects of their designs. It is compatible for different application with different physics and interfaces their combinations. COMSOL Multi-physics provides finite element methods (FEM) solution for spatial modelling. A HT-PEMFC is based on phosphoric acid doped polymer membranes that usually operates in a temperature range of 160°C to 180°C, and this section describes the 3D spatial modelling of HT-PEMFC in COMSOL as shown in Fig. 1.

It contains flow channels for the fuel (Hydrogen) and air (oxygen), gas diffusion layers (GDLs) on each side of the electrodes for the proper distribution of gases, porous electrodes (anode and cathode) where the electrochemical reactions (oxidation and reduction) takes place, membrane used as an electrolyte for ionic current flow, inlets and outlets for incoming and outgoing of hydrogen and air. The electrochemical reactions produce water on the cathode side in the cell, which lowers both partial pressures of hydrogen and oxygen on the anode and cathode, respectively and the rate of the cell reactions. The local water concentration in the cell is sometimes have positive impact because it can increase the ion conductivity, but on other hand if water condenses in the cell can cause leaching of phosphoric acid out from the polymer matrix, which can reduce the ion conducting capabilities of the membrane as well as affect performance of the whole cell. Normally water does not condensate in the cell when temperature is above 100°C, but information about water content in the porous electrodes is required to optimize shut-down procedures, during operation [6].
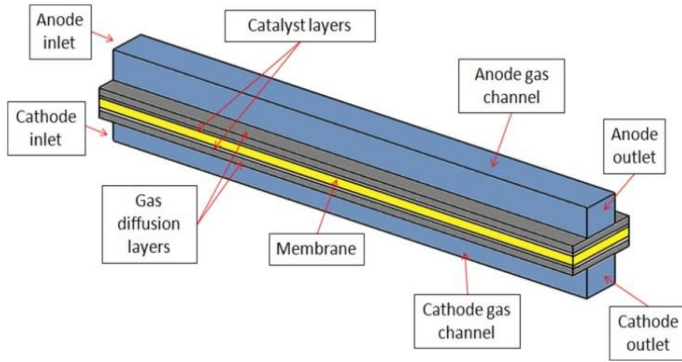
Fig. 1.   Model Geometry of HT-PEMFC [6].

The electrochemical and thermal model of HT-PEMFC consists of many sub models such as current distribution model, mass transport models in both fluid channels and in porous media, and temperature distribution model. The anode and cathode potentials are obtained by using Butler-Volmer equation and the ionic and electronic currents are calculated by Ohm's law. The mass transfer of the both reaction species in flow channels and in porous diffusion layers are calculated by Maxwell-Stefan equation. The momentum transfer in flow channels is described by the Nervier-Stokes equation whereas the momentum transfer in porous gas diffusion layers is described by the Brinkman equation. In this modelling, the different unknown variables such as electronic potential, ionic potential, hydrogen mass fraction, water mass fraction, oxygen mass fraction, nitrogen mass fraction velocity field vectors in the anode compartment, cathode compartment and also in porous media, pressure in the anode compartment cathode compartment and porous media are determined by using the above physical laws and equations. Keeping in view the system modelling as discussed in Section A, only the parameters required to be evaluated are hydrogen and air mass flow rate, which are changing with respect to change in load current. Besides this, the model is used to evaluate the performance of current distribution and potential distribution inside HT-PEMFC. The different physics used in the model to determine the unknown variables are given in the following subsections.

1) Secondary current distribution: This physics is added for modelling the electrochemical currents using Ohms law and solving for electronic potential Φs in the porous electrodes (anode and cathode) and in the GDLs, ionic potential Φl in the porous electrodes (anode and cathode), and in the electrolyte membrane. The local current densities in the porous electrodes depend on the ionic and electronic potentials, and local reactant concentrations. The hydrogen oxidation reaction occurs on the anode is given in equation 17.

$$2H_2 = 4H^+ + 4e^- \tag{17}$$

The following local current density expression (linearized concentration dependent Butler-Volmer expression) is used when no water molecules are supposed to be involved in the proton transport and the for the hydrogen oxidation reaction, then anode current density is given in equation 18.

$$i_{loc} = i_o \left(\frac{\alpha_a + \alpha_c}{RT} F \right) \eta \tag{18}$$

Where

F: Faraday's constant, 96485 [A·s·mol^{-1}],

R: Universal gas constant, 8.3145 [J·mol^{-1}K^{-1}],

T: Operating temperature of fuel cell, 453.13 [K],

α_a= 1 (Anode charge transfer coefficient),

α_c= 1, (Cathode charge transfer coefficient),

i_o = Exchange current density at anode, and it is determined by equation 19.

$$i_o = 1e^5 \ [A/m^2] \left(\frac{C_{H2}}{C_{H2,ref}} \right)^{0.5} \tag{19}$$

Where

$C_{H2, ref}$: Hydrogen reference concentration, 40.88 [mol·m^{-3}],

C_{H2}: Local hydrogen concentration [mol·m^{-3}],

Whereas, η is an activation over potential at anode and is given by equation 20.

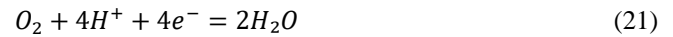$$\eta = \varphi_s - \varphi_l - E_{eq} \tag{20}$$

Where

Φ_s = Electronic potential [V]

Φ_l = Electrolyte potential [V]

E_{eq} = Equilibrium potential

The oxygen reduction reaction occurs on the cathode, known as cathode reaction in which water is produced and is given in equation 21.

$$O_2 + 4H^+ + 4e^- = 2H_2O \tag{21}$$

For the oxygen reduction reaction, the following current density expression (Catholic Tafel Equation) is used as given by equation 22.

$$\eta = A_c \times \log_{10} \left(\frac{-i_{loc}}{i_0} \right) \tag{22}$$

From above equation, current density at cathode (iloc) is determined. Whereas η is an activation over potential at cathode and is the calculated in the same as given by equation 20. The Ac is Cahtodic Tafel constant and its value should be less than 1, and here -0.095 V is considered.

The exchange current density at cathode (io), can be determined by equation 23.

$$i_o = 1 \ [A/m^2] \left(\frac{C_{O2}}{C_{O2,ref}} \right) \tag{23}$$

Where,

$C_{O2,ref}$: Oxygen reference concentration, 40.88 [mol.m^{-3}]

C_{O2}: Local oxygen concentration

The boundaries of anode GDL facing towards the flow pattern ribs are fixed to zero electronic potential, and the corresponding boundaries towards the cathode side are fixed to

the cell potential. All the other external boundaries are electrically isolating.

2) Transport of concentrated species: The Maxwell-Stefan equations are used to solve for the mass transport in the flow channels, GDLs and porous electrodes. Two Transport of Concentrated Species interfaces are used here, one for each electrode compartment. Hydrogen and water species are present on anode electrode compartment whereas oxygen, nitrogen and water are present on the cathode electrode compartment.

3) Maxwell-Stefan diffusion equations: When using Maxwell-Stefan Diffusion Model, the mass fraction of the species (wi) can be determined by equation 24.

$$\nabla . j_i + \rho(\boldsymbol{u} \cdot \nabla)w_i = R_i \qquad (24)$$

Where Ri is source term caused by chemical reactions, u is velocity field which is determined in the next physics (Free and Porous Media Flow), ρ is gas density, and can be determined by ideal gas law equation as given in equation 25.

$$\rho = \frac{p_A M_n}{RT} \qquad (25)$$

Where Mn is molar mass of the species measured in Kg/mole, R is universal gas constant, T is operating temperature of the fuel cell and pA is the absolute pressure, and is determined by equation in equation 26.

$$p_A = p + p_{ref} \qquad (26)$$

Where p is pressure which is also determined in the next physics (Free and Porous Media Flow) and pref is the reference pressure, which is taken as 101e3 [Pa] for the fuel cell. The relative mass flux vector ji for the equation 24 is calculated by using equation 27.

$$j_i = -\left(-\rho w_i \sum_k D_{ik} d_k + D_i^T \frac{\nabla T}{T}\right) \qquad (27)$$

Where Dik is the Maxwell-Stefan diffusivity matrix, measured in m²/s, and its coefficients are already described in the parameters of the fuel cell. The DiT represents the thermal diffusion coefficients of the species, measured in Kg/(m.s) but here they are not considered so their values are zero. The dk is diffusional driving force, and can be determined by equation 28.

$$d_k = \nabla x_k + \frac{1}{p_A}[(x_k - w_k)]\nabla p_A \qquad (28)$$

Where xk (mole fraction of species k) and wk (mass fraction of species k) are determined by using the equations 29 and 30.

$$x_k = \frac{w_k}{M_k}M_n \qquad (29)$$

$$M_n = \left(\sum_i \frac{w_i}{M_i}\right)^{-1} \qquad (30)$$

For determining the mass sources and sinks, the couplings are made to the secondary current distribution interface and in the same way the couplings are made to the Free and Porous Media Flow interface for evaluating the velocity field and pressure. The mass fractions are specified at the channel inlets, whereas the outflow conditions are used at channel outlets.

4) Free and porous media flow interface: The Navier-Stokes equations are used to model the velocity field and pressure (Pa) in the flow channels and Brinkman equations are used to model velocity field and pressure (Pa) in the porous gas diffusion layers (GDLs) and electrodes. The laminar inlet flow velocity profiles are considered while at the flow channel outlet boundaries, a pressure is considered. In this physics, anode and cathode compartment are made which consist of the corresponding flow channel, GDL and electrode domains. These compartments are named with "Fluid Properties" and follow the Navier-Stokes equations because of flow channels.

5) Navier-Stokes equations: The Navier-Stokes equations describe the motion of fluid substances and are derived by applying Newton's second law to fluid motion, along with the assumption that fluid stress is the sum of diffusing viscous term (proportional to the gradient of velocity) and a pressure term hence describing viscous flow. These equations explain velocity field or flow field of the fluid at a given point in space and time. The equation 31 describes how the velocity filed u is calculated.

$$\nabla \cdot (\rho u) = 0 \qquad (31)$$

Where ρ is density of species, and the dynamic viscosity μ can be taken from the material properties of the species. The pressure in flow channels can obtain by using equation 32.

$$\rho(u \cdot \nabla)u = \nabla \cdot \left[pI + \mu\big((\nabla u) + (\nabla u)^T\big) - \frac{2}{3}\mu(\nabla \cdot u)I + F\right] \quad (32)$$

Where,

I: unity matrix of order 3×3

F: Influence of gravity and other volume forces, [Kg/(m².s²)]

p: Pressure [Pa]

6) Brinkman equations: Brinkman equations have two dependent variables: the directional velocities and pressure. A combination of the continuity equation and momentum balance equation form the Brinkman equations and govern the flow in porous media. The Brinkman equations define fast-moving fluids in porous media with the kinetic potential from fluid velocity, pressure, and gravity to drive the flow. These equations are extended from Darcy's law to describe the dissipation of the kinetic energy by viscous shear as with the Navier-Stokes equations. Subsequently, this physics interface suits transitions in the best way between slow flow in porous media governed by Darcy's law and fast flow in channels described by the Navier-Stokes equations.

Porous flow is considered in "Porous Matrix Properties", which consist of anode GDL, anode electrode, cathode GDL and cathode electrode and follows the Brinkman equations. The velocity field u of the species in the porous flow is determined by equation 33.

$$\nabla . (\rho u) = Q_{br} \qquad (33)$$

Fig. 2. Modelling of HT-PEMFC System.
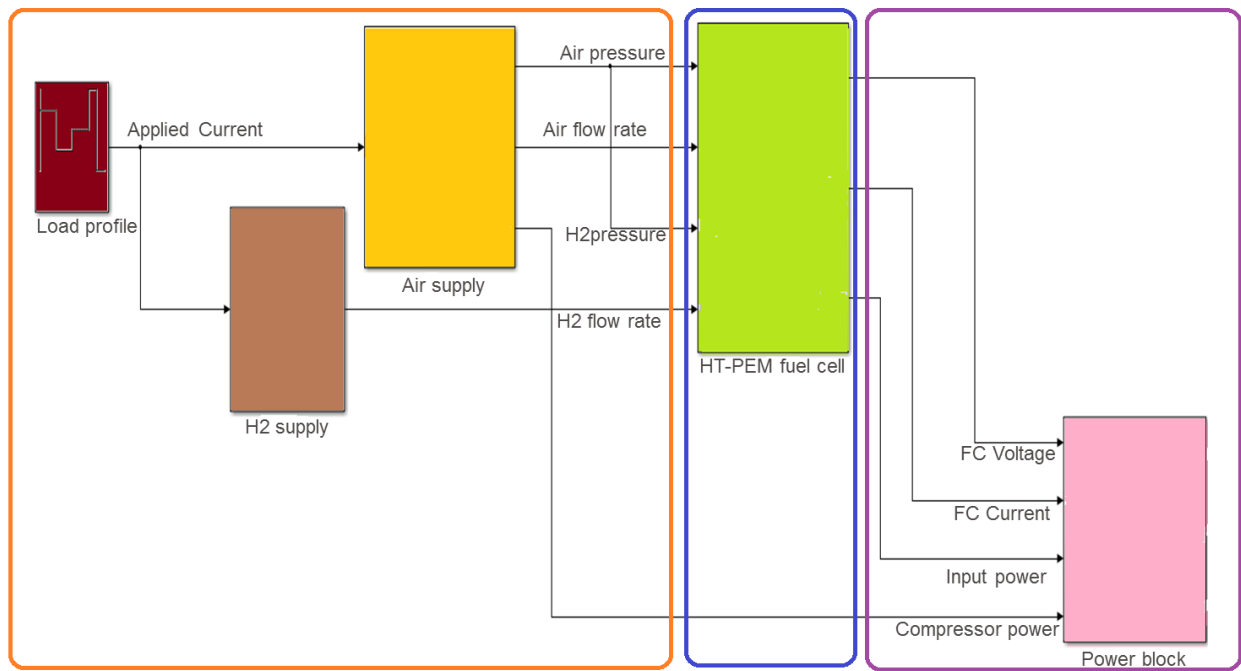
Where,

Q_{br}: Mass source or sink measured in Kg/ (m³.s)

By considering the porosity εp and the permeability Kbr [m²] of the material, the pressure of species in porous flow can be evaluated by using equation 34.

$$\frac{\rho}{\epsilon_p}\left((u.\nabla)\frac{u}{\epsilon_p}\right) = \nabla.\left[pI + \frac{\mu}{\epsilon_p}\left((\nabla u) + (\nabla u)^T\right) - \frac{2\mu}{3\epsilon_p}(\nabla.u)I\right]$$
$$-\left(\frac{\mu}{K_{br}} + \beta_F|u| + \frac{Q_{br}}{\epsilon_p^2}\right)u + F \qquad (34)$$

where β_F is Forchheimer drag option [Kg/m⁴], which adds a viscous force proportional to the square of the fluid velocity

C. Integration of spatial model with fuel with system in MATLAB/Simulink

In this section, the procedure of integration of 3D-COMSOL model with FC system is described in steps. The Fig. 2 shows the integration of 3D-COMSOL model of HT-PEMFC with the inputs and outputs blocks modelled in MATLAB/Simulink. The main objective of integration of 3D-COMSOL Model of HT-PEMFC with FC System is to observe the internal behaviours of fuel cell like voltage distribution and current distribution with the variation of load demand. First of all 3D-COMSOL model of HT-PEMFC is saved as mph file. Afterwards, the FC system model of MATLAB/Simulink is broken in to two parts in such a way that one part behaves as an input model to the 3D-COMSOL model of HT-PEMFC, whereas second part behaves as an output model that recovers the results obtained from the 3D-COMSOL of HT-PEMFC. Based on the sequence of currents and time steps taken, "for" and "if" loops are applied and the corresponding changes in voltage, power, hydrogen flow rate and air flow rate are made in the simulation results of 3D-COMSOL model of HT-

PEMFC. These results are post processed from the workspace of MATLAB in the second part of Simulink model through the same MATLAB programming. Finally, we are now able to integrate the HT-PEMFC spatial model with fuel cell (FC) System model in MATLAB/Simulink by using COMSOL LiveLink for MATLAB.

III. SIMULATION RESULTS OF HT-PEMFC SYSTEM

This section describes the results into the following two subsections as obtained from MATLAB/Simulink model of the HT-PEMFC system model and internal behaviours of 3D-COMSOL model of HT-PEMFC.

A. MATLAB Results

These results are obtained from MATLAB by integrating the HT-PEMFC COMSOL Model. Since the integration process is already mentioned that consists of input and output models. The results of both the models are given in Fig. 3 and Fig. 4, respectively.

Fig. 3 represents four parameters namely load current [A], current density [A/m²], H2 flow rate [m³/sec] and O2 flow rate [m³/sec] from top y-axis to bottom y-axis respectively. It shows that how the parameters like hydrogen flow rate and air flow rate are varied as the load current changes with respect to time on x-axis. The load in the model is considered as a dynamic load applied at different time steps. The total time of simulation is 4 seconds with the 400 time steps, means each time step is of 0.01 second and the value of the load current is assigned to each time step. The dynamic load current is applied in such a way that for each 80 time steps it varies with time. For the first 80 time steps, the load current 0.06 A is considered, and for the remaining each 80 steps 0.04 A, 0.05 A, 0.07 A, and 0.03 A of the load current is considered. The current density is obtained by simply dividing the load current

by the fuel cell current collecting area. The air and hydrogen flow rates change from the air compressor and fuel supply system respectively in accordance with change in load current as described in Section II. Here the important thing to be noticed is the compressor dynamics of the air compressor, which is considered here as 0.1 second.

Fig. 4 illustrates the results achieved from the COMSOL after integrating as described above. The output voltage, output power, utilization and efficiency of the fuel cell are presented on y-axis from top to bottom respectively. As the load current changes shown in the input model results in Fig. 3, the corresponding changes in output voltage, output power, utilization and efficiency of the fuel cell occurs as shown in Fig. 4. An increase in load current is followed by an increase in output power because the output power of the fuel cell is multiplication of the load current drawn from the fuel cell and output voltage of the fuel cell. In the same way higher the output power obtained from the fuel cell, higher will be the input power required. On the other hand the sudden increase in load current causes decrease in the output voltage and efficiency of the fuel cell, because the delay of compressor causes depletion of oxygen for the reaction so the output

voltage and hence the efficiency of fuel cell decrease. While the hydrogen utilization of the fuel cell is almost constant because as the load current changes, so the fuel flow rate changes.

B. COMSOL Results

These results are very important and interesting too because they show the internal behavior of the fuel cell varying with respect to the dynamics of load current. The COMSOL results are obtained by putting the values as an input values to the COMSOL model of HT-PEMFC. Four case studies have been done for observing the distribution of electric potential and current density on cathode at time 2.39 seconds, and 2.45 seconds. These time steps are further marked with red circle for clear understanding of time steps taken for simulation in Fig. 4. These time steps are taken in such a way to observe the changes occurring in the internal behaviour of the fuel cell when there occurs a sudden increase in the load current from 0.05 A (at t=2.39 seconds) to 0.07 A (at t=2.45 seconds). In all these figures of COMSOL results, the cut plane view of cathode electrode of 3D-COMSOL model of HT-PEMFC is taken. The x-axis and y-axis of this 2D plot represent the width and length of cathode electrode.
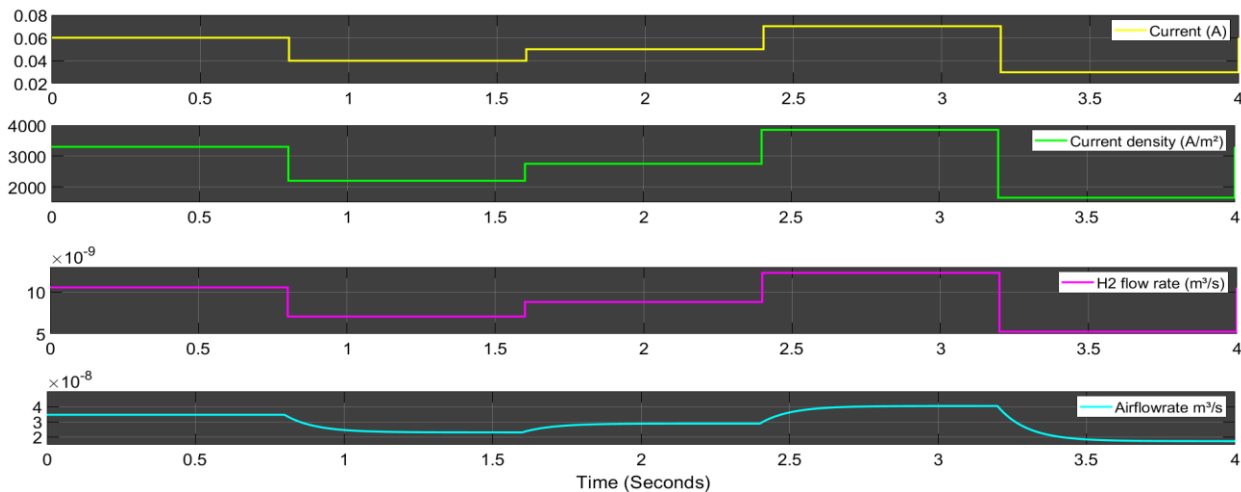

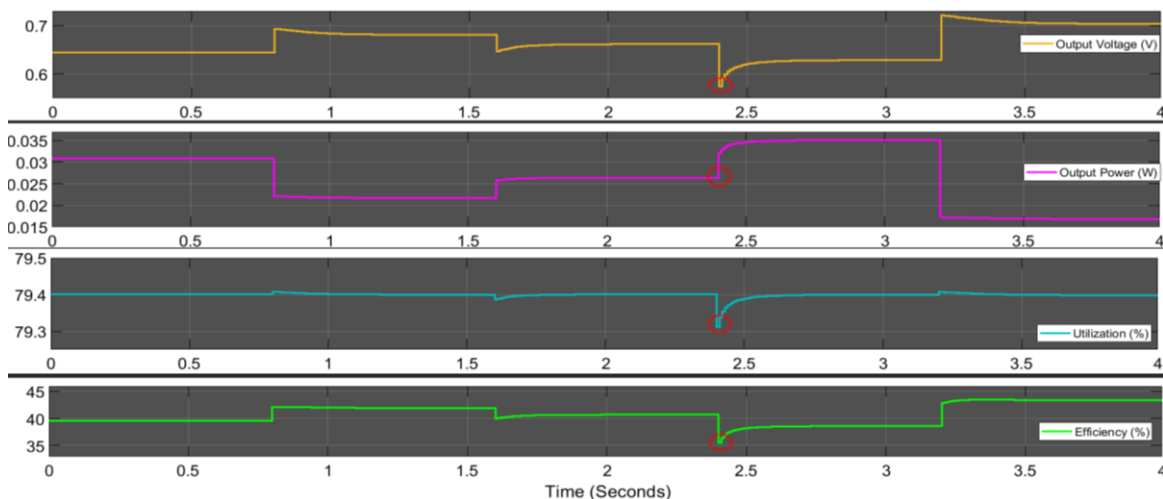Fig. 3. Inputs from MATLAB model to HT-PEMFC CSOMSOL Model

Fig. 4. Outputs from HT-PEMFC CSOMSOL Model.

1) Case 1: electric potential (At t=2.39 seconds): In Fig. 5, the minimum value of electric potential is 0.6608 V and the maximum value is 0.6644 V. The maximum value is at the centre of the x-axis and it decreases along the y-axis as moving from the inlet to outlet. The value does not change so much at the centre of the x- but changes very rapidly at the edges. As we move away from the centre of x-axis towards the left or right side the value of electric potential decreases because the concentration of the reactant is higher at the centre and lower at the edges.

2) Case 2: electric potential (at t=2.45 seconds): In Fig. 6, the minimum value of electric potential is 0.6118 V and the maximum value is 0.6173 V. The value of electric potential decreases along the y-axis as moving from the inlet to outlet. The value does not change so much at the centre of the x-axis and is maximum that is 0.6173 V but changes very rapidly at the edges. As we move away from the centre of x-axis towards the left or right side the value of electric potential decreases because the concentration of the reactant is higher at the centre and lower at the edges. Here the electric potential is lower as compared to case 1; the reason is same that is a sudden increase in current causes decrease in the electric potential. On the other hand electric potential in this case is almost same as compared to case 2 because at this time step, the same current is drawn which is 0.07 A.
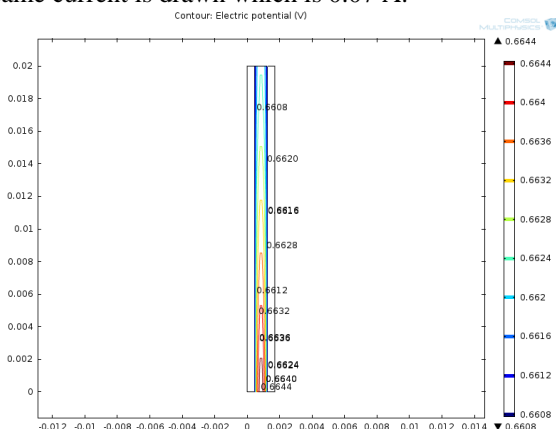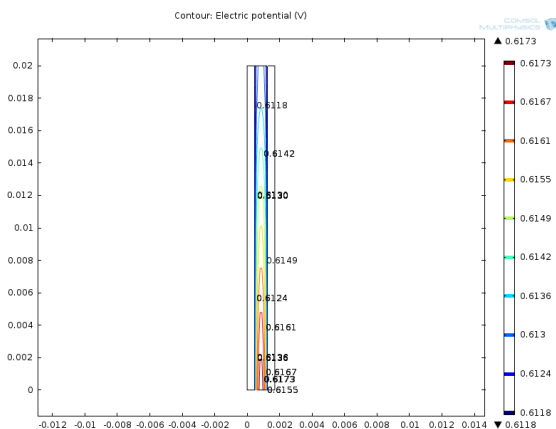
3) Case 3: electrode current density (at t=2.39 seconds): In Fig. 7, the minimum value of electrode current density is 471.82 A/m² at the centre of the x-axis. If we move away from the x-axis towards the left or right side from the centre of x-axis, the value of electrode current density increases up to the maximum value that is 6347.4 A/m² and afterwards it again decreases up to the average value of 2675.2 A/m² at the edges of the electrodes. The important point to be noted here is that the current distribution at the inlet is too much whereas at the outlet is very low. The maximum current distribution at the outlet is at the centre of the x-axis that is 3409.6 A/m² and 1206.3 A/m² at outlet edges.

4) Case 4: electrode current density (at t=2.45 seconds): In Fig. 8, the minimum value of electrode current density is 672.93 A/m² at the centre of the x-axis. As we move away from the x-axis towards the left or right side from the centre of x-axis, the value of electrode current density increases up to the maximum value that is 9763.6 A/m² and afterwards it again decreases up to the average value of 7490.9 A/m² at the edges of the electrodes. The important point to be noted here is that the current distribution at the inlet is too much whereas at the outlet is very low. The current distribution at the outlet of the centre of the x-axis is 1809.3 A/m².
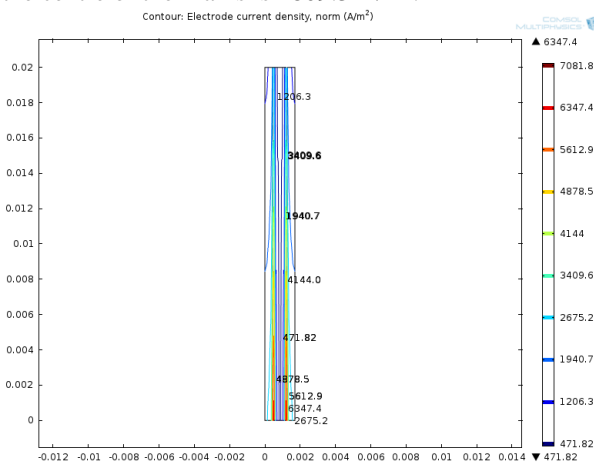

Fig. 5. Case 1: Electric Potential.

Fig. 7. Case 3: Electrode Current Density.
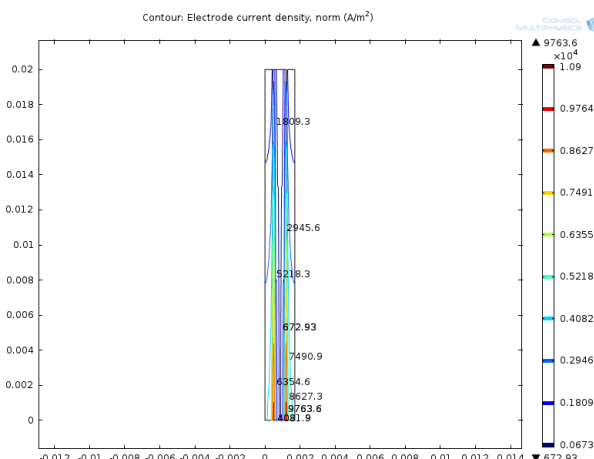

Fig. 6. Case 2: Electric Potential.

Fig. 8. Case 4: Electrode Current Density.

IV. CONCLUSION

This paper proposes a solution to observe the internal behaviour of fuel cell like voltage distribution, current distribution with the variation of load demand integration of 3D-COMSOL Model of HT-PEMFC with FC System. The task of achieving the effects of the load variation on HT-PEMFC has been achieved along with the internal behaviour of the fuel cell. The current findings with this approach of modelling can be useful to examine performance of HT-PEMFC in a better and accurate way. Moreover integration of HT-PEMFC with MATLAB allows more flexibility of changing any parameter with the M-script file, thus helps to find out more results as required. The result shows that concentration of electric potential and electrode current density distribution have adverse effects at the centre and edges cathode electrode of HT-PEMFC. The HTPEM-FC system does not include the thermal model, so thermal effects are not considered. In future work the thermal model can be added into HTPEM-FC system and the effects of temperature distribution on performance of the HTPEM-FC can be achieved. Since in practice HTPEM-FC contains stack were number of cells are connected together in series and parallel combination to obtain the desired power. This research work can be further helpful to replace the single cell with stack, and also replace single channels of gases with multiple channels to achieve the required power.

ACKNOWLEDGMENT

REFERENCES

[1] J. Zhang et al., "High temperature PEM fuel cells," Journal of Power Sources, vol. 160, no. 2 SPEC. ISS., pp. 872–891, 2006.

[2] Y. Wang, K. S. Chen, J. Mishler, S. C. Cho, and X. C. Adroher, "A review of polymer electrolyte membrane fuel cells: Technology, applications, and needs on fundamental research," Applied Energy, vol. 88, no. 4, pp. 981–1007, 2011.

[3] S. Sharma and B. G. Pollet, "Support materials for PEMFC and DMFC electrocatalysts - A review," Journal of Power Sources, vol. 208, pp. 96–119, 2012.

[4] A. Chandan et al., "High temperature (HT) polymer electrolyte membrane fuel cells (PEMFC)-A review," Journal of Power Sources, vol. 231, pp. 264–278, 2013.

[5] R. E. Rosli et al., "A review of high-temperature proton exchange membrane fuel cell (HT-PEMFC) system," International Journal of Hydrogen Energy, vol. 42, no. 14, pp. 9293–9314, 2017.

[6] R. K. Abdul Rasheed, Q. Liao, Z. Caizhi, and S. H. Chan, "A review on modelling of high temperature proton exchange membrane fuel cells (HT-PEMFCs)," International Journal of Hydrogen Energy, vol. 42, no. 5, pp. 3142–3165, 2017.

[7] A. YMERI and S. MUJOVIC, "Impact of Photovoltaic Systems Placement, Sizing on Power Quality in Distribution Network," Advances in Electrical and Computer Engineering, vol. 18, no. 4, pp. 107–112, Dec. 2018.

[8] J. A. Laghari, S. Ahmed, J. Kumar, and H. Mokhlis, "A Smart Under-Frequency Load Shedding Scheme based on Takagi-Sugeno Fuzzy Inference System and Flexible Load Priority," Int. J. Adv. Comput. Sci. Appl., vol. 9, no. 3, 2018.

[9] Q. Yan, H. Toghiani, and H. Causey, "Steady state and dynamic performance of proton exchange membrane fuel cells (PEMFCs) under various operating conditions and load changes," Journal of Power Sources, vol. 161, no. 1, pp. 492–502, 2006.

[10] W. Andari, S. Ghozzi, H. Allagui, and A. Mami, "Design, Modeling and Energy Management of a PEM Fuel Cell / Supercapacitor Hybrid Vehicle," Int. J. Adv. Comput. Sci. Appl., vol. 8, no. 1, pp. 273–278, 2017.

[11] H. CHAOUALI, H. OTHMANI, M. Selméne, D. MEZGHANI, and A. MAMI, "Energy Management Strategy of a PV/Fuel Cell/Supercapacitor Hybrid Source Feeding an off-Grid Pumping Station," Int. J. Adv. Comput. Sci. Appl., vol. 8, no. 8, pp. 250–257, 2017.

[12] B. Mebarki, B. Allaoua, B. Draoui, and D. Belatrache, "Study of the energy performance of a PEM fuel cell vehicle," International Journal of Renewable Energy Research, vol. 7, no. 3, 2017.

[13] J. Kumar, L. Kumpulainen, and K. Kauhaniemi, "Technical design aspects of harbour area grid for shore to ship power: State of the art and future solutions," International Journal of Electrical Power & Energy Systems, vol. 104, no. June 2018, pp. 840–852, Jan. 2019.

[14] A. TOFIGHI and A. KALANTAR, "Adaptive Passivity-Based Control of PEM Fuel Cell/Battery Hybrid Power Source for Stand-Alone Applications," Advances in Electrical and Computer Engineering, vol. 10, no. 4, pp. 111–120, 2010.

[15] Y. K. RENANI, B. VAHIDI, and H. A. ABYANEH, "Effects of Photovoltaic and Fuel Cell Hybrid System on Distribution Network Considering the Voltage Limits," Advances in Electrical and Computer Engineering, vol. 10, no. 4, pp. 143–148, 2010.

[16] Y. Wang, J. Kowal, and D. U. Sauer, "Modeling of HTPEM Fuel Cell Start-Up Process by Using Comsol Multiphysics Principle of PEM fuel cell," Comsol Conference, no. June 2015, 2012.

[17] Q. Li, W. Chen, Y.-T. Cham, M. Han, and J. Jia, "Dynamic characteristic modeling and control of proton exchange membrane fuel cell," Xinan Jiaotong Daxue Xuebao/Journal of Southwest Jiaotong University, vol. 44, no. 4, pp. 604–608, 2009.

[18] I. P. Sahu, G. Krishna, M. Biswas, and M. K. Das, "Performance study of PEM fuel cell under different loading conditions," Energy Procedia, vol. 54, pp. 468–478, 2014.

[19] C. Zhang, Z. Liu, X. Zhang, S. H. Chan, and Y. Wang, "Dynamic performance of a high-temperature PEM (proton exchange membrane) fuel cell - Modelling and fuzzy control of purging process," Energy, vol. 95, pp. 425–432, 2016.

[20] L. Xia et al., "Investigation of parameter effects on the performance of high-temperature PEM fuel cell," International Journal of Hydrogen Energy, vol. 3, 2018.

[21] J. Ma and M. Baysal, "Online Energy Management Strategy Based on Adaptive Model Predictive Control for Microgrid with Hydrogen Storage," vol. 8, no. 2, 2018.

[22] Y. Allahvirdizadeh, M. Mohamadian, and M.-R. HaghiFam, "A comparative study of energy control strategies for a standalone PV/WT/FC hybrid renewable system," International Journal of Renewable Energy Research (IJRER), vol. 7, no. 3, pp. 1463–1475, 2017.

[23] Y. Wang, D. U. Sauer, S. Koehne, and A. Ersöz, "Dynamic modeling of high temperature PEM fuel cell start-up process," International Journal of Hydrogen Energy, vol. 39, no. 33, pp. 19067–19078, 2014.